

## Article

# Elastic Flexibility in an Optically Active Naphthalidenimine-Based Single Crystal

Torvid Feiler<sup>1,2</sup>, Adam A. L. Michalchuk<sup>1</sup> , Vincent Schröder<sup>3,4</sup>, Emil List-Kratochvil<sup>3,4</sup>, Franziska Emmerling<sup>1,2,\*</sup>  and Biswajit Bhattacharya<sup>1,\*</sup> 

<sup>1</sup> BAM Federal Institute for Materials Research and Testing, Richard-Willstätter-Str. 11, 12489 Berlin, Germany; torvid.feiler@bam.de (T.F.); adam.michalchuk@bam.de (A.A.L.M.)

<sup>2</sup> Department of Chemistry, Humboldt-Universität zu Berlin, Brook-Taylor-Str. 2, 12489 Berlin, Germany

<sup>3</sup> Department of Chemistry, Department of Physics, and IRIS Adlershof, Humboldt-Universität zu Berlin, Zum Großen Windkanal 2, 12489 Berlin, Germany; vincent.schroeder@helmholtz-berlin.de (V.S.); emil.list-kratochvil@hu-berlin.de (E.L.-K.)

<sup>4</sup> Helmholtz-Zentrum Berlin für Materialien und Energie GmbH, Hahn-Meitner-Platz 1, 14109 Berlin, Germany

\* Correspondence: franziska.emmerling@bam.de (F.E.); biswajit.bhattacharya@bam.de (B.B.)

**Abstract:** Organic single crystals that combine mechanical flexibility and optical properties are important for developing flexible optical devices, but examples of such crystals remain scarce. Both mechanical flexibility and optical activity depend on the underlying crystal packing and the nature of the intermolecular interactions present in the solid state. Hence, both properties can be expected to be tunable by small chemical modifications to the organic molecule. By incorporating a chlorine atom, a reportedly mechanically flexible crystal of (E)-1-(4-bromo-phenyl)iminomethyl-2-hydroxyl-naphthalene (BPIN) produces (E)-1-(4-bromo-2-chloro-phenyl)iminomethyl-2-hydroxyl-naphthalene (BCPIN). BCPIN crystals show elastic bending similar to BPIN upon mechanical stress, but exhibit a remarkable difference in their optical properties as a result of the chemical modification to the backbone of the organic molecule. This work thus demonstrates that the optical properties and mechanical flexibility of molecular materials can, in principle, be tuned independently.

**Keywords:** crystal engineering; molecular crystal; mechanical property; elastic crystal



**Citation:** Feiler, T.; Michalchuk, A.A.L.; Schröder, V.; List-Kratochvil, E.; Emmerling, F.; Bhattacharya, B. Elastic Flexibility in an Optically Active Naphthalidenimine-Based Single Crystal. *Crystals* **2021**, *11*, 1397. <https://doi.org/10.3390/cryst11111397>

Academic Editor: Ana M. Garcia-Deibe

Received: 30 October 2021

Accepted: 13 November 2021

Published: 16 November 2021

**Publisher's Note:** MDPI stays neutral with regard to jurisdictional claims in published maps and institutional affiliations.



**Copyright:** © 2021 by the authors. Licensee MDPI, Basel, Switzerland. This article is an open access article distributed under the terms and conditions of the Creative Commons Attribution (CC BY) license (<https://creativecommons.org/licenses/by/4.0/>).

## 1. Introduction

Crystalline materials are usually brittle and are prone to breaking when mechanically stressed. This behavior greatly limits the application of single crystals as the next generation of adaptable, functional materials. The recent discovery of mechanical compliancy in molecular crystals has demonstrated that small molecules can combine the advantages of crystalline materials (e.g., optical emission, piezoelectricity, and light polarization) with the adaptivity of soft matter [1–10]. Such materials show exceptional promise for promoting new technologies, with their potential already being shown in their use as micro-optoelectronic devices [11,12], sensors [13,14], biomimetics [15,16], and as optical waveguides [17–20].

Based on the reversibility of the deformation, molecular crystals can be defined as being plastically (irreversibly) or elastically (reversibly) bendable [1,21–23]. Plastic bending is generally associated with anisotropic interactions within the crystal packing and the presence of low energy slip planes [2,4]. In contrast, isotropic interactions, together with weak and dispersive interactions (halogen bonding and van der Waals interactions), are related to mechanical elasticity [5,21,23]. These weak interactions can act as ‘structural buffers’, ensuring that the molecules return to their equilibrium geometry after releasing the mechanical stress [21]. Depending on the technological application one has in mind, a particular mechanical regime may be necessary. For example, reusable sensors must be based on elastically flexible materials [24,25], whereas shapable electronics can be prepared

from plastically flexible crystals [26]. Correspondingly, developing an understanding of the flexible, functional materials in both mechanical regimes is necessary for targeting real-world applications [27,28].

In addition to designing mechanical flexibility, strategies for coupling flexibility with a functional property are necessary. Consequently, growing efforts have been devoted towards strategies for imparting flexibility in materials with a desired functionality [25,29]. Strategies that are based on selective polymorphism or cocrystallization are promising as they do not require any chemical modification of the functional molecule [7,30,31]. However, such strategies are greatly limited by the propensity of the desired molecule for polymorphism or cocrystallization and the unpredictable availability of suitable crystallographic packing in these new crystal forms. Instead, more successful strategies are based on the functionalization of active molecules using functional groups that are known to generate the crystallographic features necessary for flexibility [8,32]. Often, this takes the form of introducing 'soft spherical' moieties, such as methyl or halogen groups [4,33]. In this way, one, in principle, simultaneously tunes both the mechanical and functional properties of the system.

To this end, the present study explores the possibility of influencing the mechanical and optical properties of the reportedly mechanically flexible crystal (E)-1-(4-bromophenyl)iminomethyl-2-hydroxyl-naphthalene (BPIN) [34]. With well-defined chromophores, BPIN offers an excellent opportunity to consider how chemical modification can influence both mechanical and optical properties. In this work, we chemically modified the phenyl ring of BPIN by introducing another chlorine atom in order to synthesize (E)-1-(4-bromo-2-chloro-phenyl)iminomethyl-2-hydroxyl-naphthalene (BCPIN). The incorporation of a 'soft spherical' moiety in the optically active flexible crystal ensures prominent mechanical flexibility. This molecule has significant potential for exploring the simultaneous effects resulting from chemical modification to the optical and mechanical properties of molecular materials.

## 2. Experimental Section

### 2.1. Materials

4-Bromo-2-chloroaniline (99.51%) and 2-hydroxy-1-naphthaldehyde (98%) were purchased from BLDpharm (Kaiserslautern, Germany) and abcr (Karlsruhe, Germany), respectively, and used as received.

### 2.2. Synthesis and Crystal Growth

(E)-1-(4-bromo-2-chloro-phenyl)iminomethyl-2-hydroxyl-naphthalene (BCPIN) was synthesized in a mechanochemical reaction between a stoichiometric mixture of 2-hydroxy-1-naphthaldehyde (1 mmol, 172 mg) and 4-bromo-2-chloroaniline (1 mmol, 206 mg) by using a mortar and pestle with the addition of ca. 500  $\mu$ L of methanol. The obtained powder was dissolved in 15 mL of dichloromethane (DCM). In a test tube, 6 mL of ethanol was carefully layered on top of the 2 mL of the DCM solution, so that a phase boundary was obtained. The mixture was then left to crystallize. After the slow evaporation of the solvents, small needle-shaped crystals were obtained.

### 2.3. Single-Crystal X-Ray Diffraction (SCXRD)

Single crystal X-ray diffraction (SCXRD) data from BCPIN were collected using a Bruker D8 Venture diffractometer (Bruker AXS, Karlsruhe, Germany) equipped with graphite-monochromated Mo  $K_{\alpha}$  radiation ( $\lambda = 0.71073$  Å). The data reduction was performed using the Bruker AXS SAINT [35] and SADABS [36] software packages. Both structures were solved by SHELXT 2018 [37] using direct methods, followed by successive Fourier and difference Fourier syntheses. Full-matrix least-squares refinements were carried out on  $F^2$  using SHELXL 2018 [38], including the anisotropic displacement parameters for all of the non-hydrogen atoms. The hydrogen atoms that were bonded to oxygen were located using the electron density maps, and all of the hydrogen atoms that were

bonded directly to carbon atoms were fixed at their ideal positions. The data collection methods, structure-refinement parameters, and crystallographic data of the cocrystals are summarized in Table S1.

#### Powder X-Ray Diffraction (PXRD)

The ground crystals were packed into borosilicate capillaries with an inner diameter of 0.5 mm. PXRD data were collected on a Bruker D8 Discover diffractometer (Bruker AXS, Karlsruhe, Germany) equipped with a LYNXEYE XE detector and Cu  $K_{\alpha 1}$  radiation ( $\lambda = 1.5406 \text{ \AA}$ ). Data were collected over a range of  $2\theta = 3^\circ$  to  $50^\circ$ , with step size of  $0.009^\circ$  and 6 s per step. The comparison between the simulated and experimental PXRD patterns is depicted in Figure S1.

#### 2.4. Differential Scanning Calorimetry (DSC)

The differential scanning calorimetry (DSC) measurements were performed with a TGA/DSC 3+ (Mettler Toledo, Greifensee, Switzerland). The measurements were performed in open aluminum crucibles under continuous  $N_2$ -air flow. The experiments were conducted at a heating rate of 5 K/min, in a range from  $25^\circ\text{C}$  to  $200^\circ\text{C}$ . The DSC plot of the BCPIN crystal is presented in Figure S2.

#### 2.5. Photoluminescence Spectroscopy

The photoluminescence measurements were performed with an Edinburgh Instruments FLS 980 fluorescence spectrometer (Livingston, UK). All photoluminescence spectra were measured in an integrating sphere. The samples were excited with a 450 W ozone-free xenon arc lamp. The detector was a R928P PMT and electrically cooled to  $-20^\circ\text{C}$ .

#### 2.6. Electronic Band Structure

The electronic band structure was calculated within the framework of density functional theory as implemented in CRYSTAL17 [39]. Atom-centered Gaussian basis sets were used for each atom, using the pob\_TZVP\_rev2 basis sets published by Vilela Oliveira et al. [40]. The electronic structure was calculated by using the screened hybrid functional of Heyd–Scuseria–Ernzerhof (HSE06) [41], which has previously been shown to provide excellent agreement with the experimental optical band gaps of molecular solids [42]. The electronic structure was sampled using a shrinking factor of 7 and Coulomb and exchange integral tolerances of 7, 7, 7, 9 and 30.

### 3. Results and Discussion

#### 3.1. Crystal Structure

BCPIN crystallizes in the monoclinic space group  $P2_1/c$ , with one molecule in the asymmetric unit (Figure S4). Crystal face indexing by single crystal X-ray diffraction shows that the two major faces of BCPIN crystals are the (010)/(0 $\bar{1}$ 0) and (001)/(00 $\bar{1}$ ) faces, with the minor face being the (100)/( $\bar{1}$ 00) face (Figures 1a and S3). The molecule comprises an intramolecular hydrogen-bonding interaction (O-H $\cdots$ N; 1.81  $\text{\AA}$ ) between the CH=N and OH groups, which results in a slight twisting of the phenyl rings out of the CH=N plane by a torsional angle of  $35.64^\circ$  (Figure 1a, inset). Molecules are connected through the C-H $\cdots$ Cl (2.909) and C-H $\cdots$ O (2.439  $\text{\AA}$ ) interactions along the crystallographic  $c$ -axis (Figure 1a). Herringboned chains are formed by C-H $\cdots$ Br interactions (2.97  $\text{\AA}$ ) along the crystallographic  $b$ -axis (Figure 1a), interacting further along the  $a$ -axis through  $\pi\cdots\pi$  stacking (3.83  $\text{\AA}$ ).

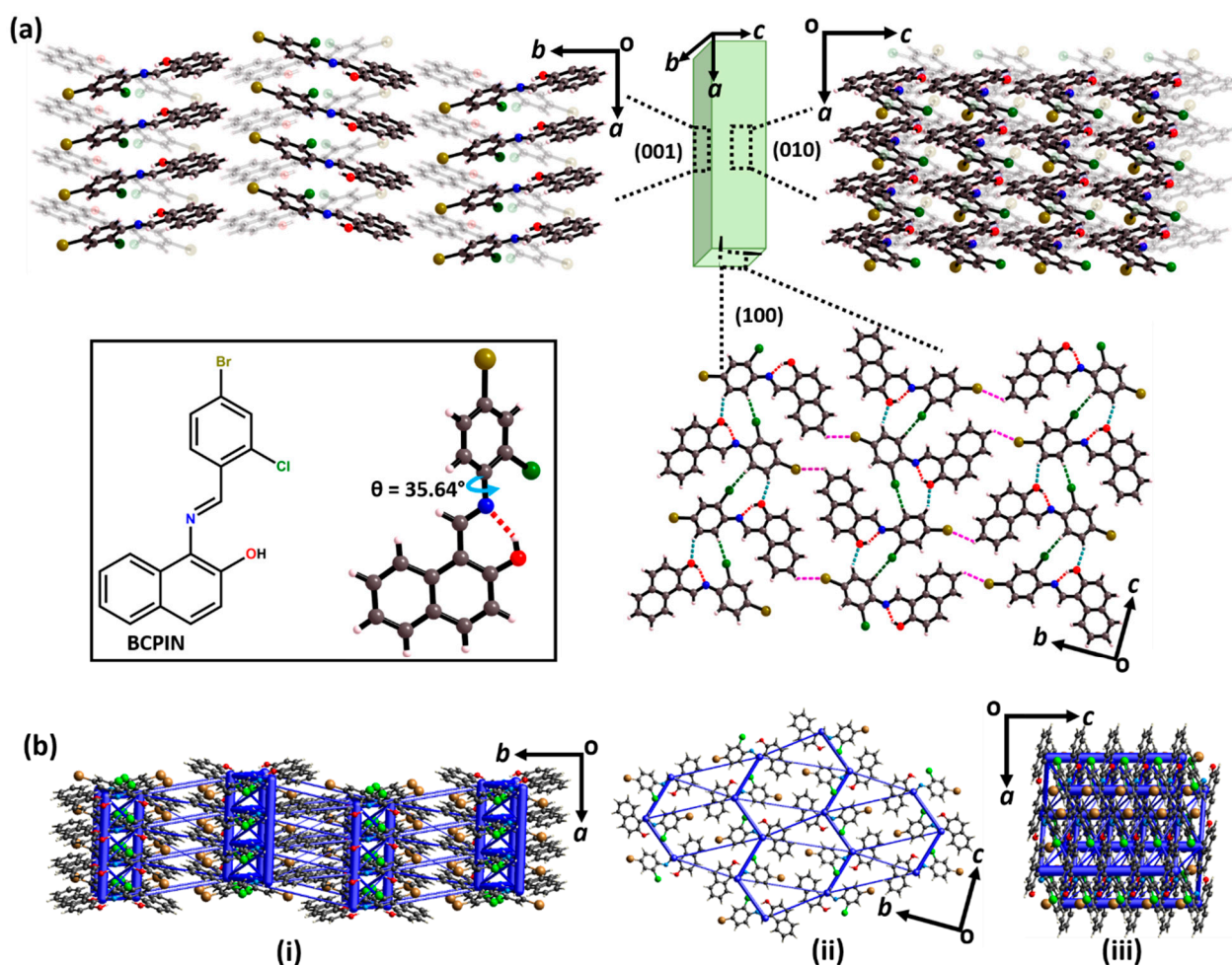


**Figure 1.** (a) Crystal packing in (E)-1-(4-bromo-2-chloro-phenyl)iminomethyl-2-hydroxyl-naphthalene (BCPIN). View of molecular arrangement on (001), (100), and (010) faces. The view of intermolecular interactions present in the crystal packing of BCPIN (O–H···N interactions: red dotted lines, C–H···O interactions: cyan dotted lines, C–H···Cl interactions: green dotted lines and C–H···Br interactions: magenta dotted lines). The molecular formula of BCPIN and molecular conformation are shown as an inset. (b) Energy frameworks showing the total intermolecular interactions energy (blue) viewed along the *c*-axis (i), *a*-axis (ii), and *b*-axis (iii). The line thickness represents the magnitude of energy (line size 100 and energy cut-off  $5 \text{ kJ}\cdot\text{mol}^{-1}$ ).

As established in recent trends in the crystal engineering of mechanically flexible materials, the herringbone motif and the absence of slip planes within the crystal structure of BCPIN suggest that the material may exhibit a notable elastic regime. This assumption is also supported by the results of the energy framework calculation [43]; Figures 1b and S5. The interactions along the crystallographic *a*-axis are ca.  $58.8 \text{ kJ}\cdot\text{mol}^{-1}$ , with those along the *c* and *b*-axes being ca.  $53.4 \text{ kJ}\cdot\text{mol}^{-1}$  and  $31.8 \text{ kJ}\cdot\text{mol}^{-1}$ , respectively. These reveal the quasi-isotropic interactions that are conventional for elastic flexibility (Table S2) [44,45].

The mechanical properties of BCPIN were tested by three-point bending experiments, in which forceps held the crystal at either end while a needle exerted a force between them. This revealed a remarkable degree of elasticity when the crystal was pushed along the (010) face (Figure 2a). Moreover, the bending was repeatable over several cycles without visible crystal fractures, confirming macroscopic reversibility. Our measurements suggest that there is an elastic strain of  $\epsilon \approx 2.70\%$  for BCPIN (Figure S6). In contrast, when force was applied over the (001) face, crystal fracture was observed (Figure 2b).

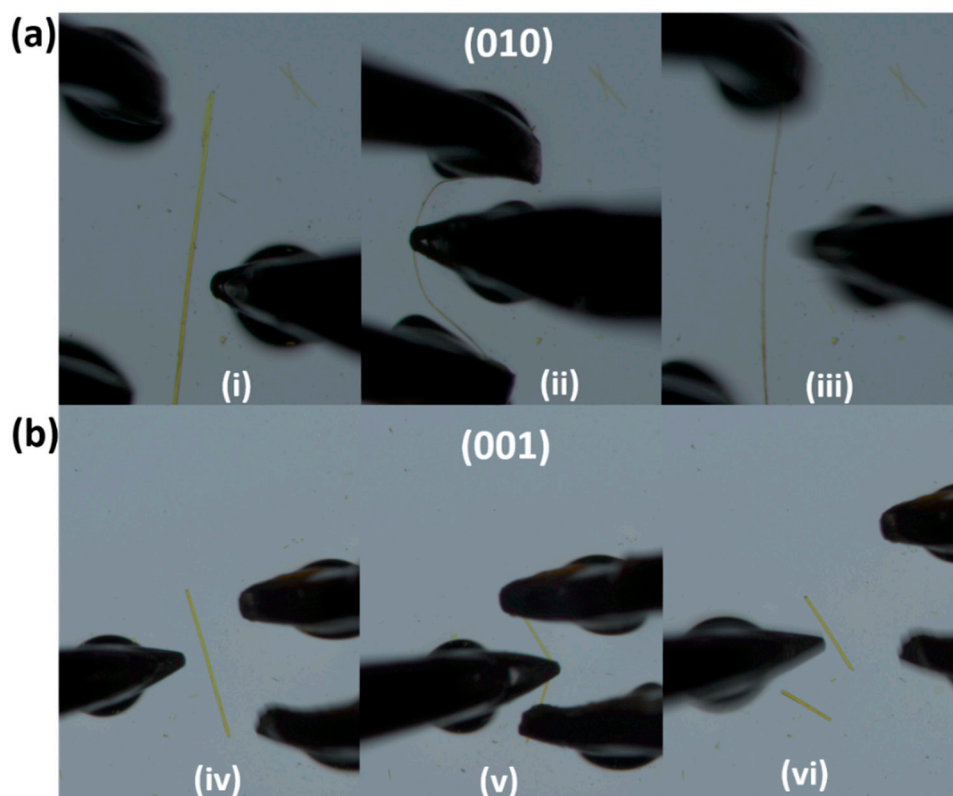


**Figure 2.** Optical microscope photographs of (a) elastic bending, and (b) brittle fracture of BCPIN crystal over (010) and (001) crystallographic faces upon mechanical stress, respectively.

Microfocus X-ray diffraction experiments have suggested that elastic bending causes the simultaneous expansion and contraction of the outer and inner arcs, respectively, along the long axis of a crystal [5,23]. For BCPIN, this corresponds to the compression/expansion of the  $\pi\cdots\pi$  interactions. Assuming linear elasticity and  $\epsilon \approx 2.70\%$ , one can approximate that the maximum expansion and contraction of the  $a$ -axis is  $\pm 0.10$  Å. As 3.83 Å approaches the upper limit for the conventional  $\pi$ -stacking criteria, we can propose that material fractures, caused by bending beyond the elastic limit, are correlated with the overextension of the  $\pi\cdots\pi$  distance [17].

### 3.2. Optical Properties

The presence of the naphthalene chromophore and  $\pi\cdots\pi$  interactions in the solid state of BCPIN crystal prompted us to investigate the optical properties for potential applications in flexible optical devices. Unfortunately, in monoclinic crystals the crystal surfaces are not related by symmetry. This gives rise to anisotropic physical properties and complicates the measurement of the material's optical behavior in single crystals. To overcome this complication, we performed photoluminescence (PL) measurements on powdered samples of BCPIN. A combination of X-ray powder diffraction and differential scanning calorimetry confirmed that grinding did not alter the crystallographic form of BCPIN (Figures S1 and S2).

The solid-state PL spectrum measured with 410 nm excitation revealed maxima at 480 and 545 nm. Correspondingly, the solid-state photoluminescence excitation (PLE) spectra were measured using the photoluminescence intensity at each of these characteristic wavelengths, as shown in Figure 3a. The PLE spectrum measured at 480 nm revealed a single maximum at 422 nm, presumably indicating the resonant absorption energy of the material. Our *ab initio* band structure calculations, using the HSE06 functional, do indeed suggest a fundamental electronic band gap at 426.06 nm (2.91 eV). We note that the optical band gap that is measured by spectroscopy is expected to be somewhat lower in energy

than the fundamental gap calculated by DFT. We, therefore, expect that the exceptional agreement between the two may result from a fortuitous cancellation of errors. The PLE spectrum measured at 560 nm, shown in black in Figure 3b, shows three maxima instead: 428 nm, 444 nm, and 500 nm. As the emission of BCPIN (the red line in Figure 3a) overlaps with the low energy part of the PLE spectra (the black line in Figure 3a), self-absorption presumably takes place. This may explain the low quantum yield of BCPIN ( $\Phi < 0.1\%$ ). This also reduces the intensity of the signal at 480 nm and, at the same time, makes the signal at 545 nm more intense.

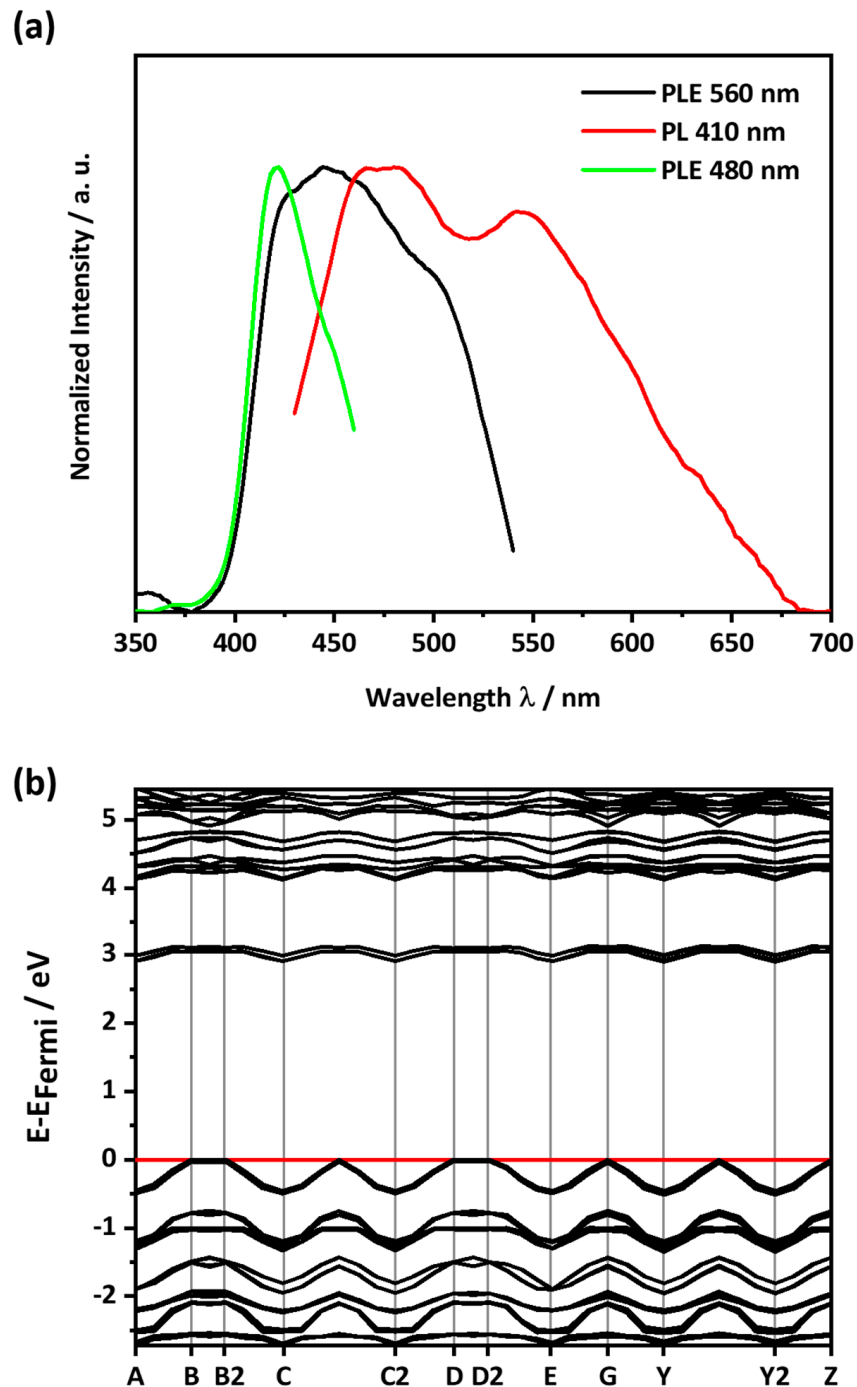


**Figure 3.** (a) Solid-state photoluminescence (PL, red line) and photoluminescence excitation (PLE, green line and black line) spectra of BCPIN. (b) Simulated band structure of BCPIN as obtained at HSE06 level of theory.

A comparison of the BCPIN optical spectra with those of (E)-1-(4-bromo)iminomethyl-2-hydroxyl-naphthalene (BPIN) [34] shows that the additional chlorine atom exerts a marked influence on the electronic structure of the molecule. The photoluminescence spectrum of BPIN only shows a single maximum (536 nm), in contrast to the dual maxima (480 and 545 nm) observed for BCPIN. Therefore, we can observe a significant change in the emission profile due to this chemical change. In addition, a blue shift of about 60 nm can be seen for the emission maximum. At the same time, increased self-absorption is observed in BCPIN. It, therefore, appears that the addition of the Cl atom onto the molecular backbone leads to a significant increase in the specificity of the optical activity of the flexible material, without modifying the elastic behavior.

#### 4. Conclusions

We successfully synthesized a new flexible crystal based on (E)-1-(4-bromo-2-chlorophenyl)iminomethyl-2-hydroxyl-naphthalene (BCPIN). Single crystals of BCPIN exhibit marked bulk elastic flexibility ( $\epsilon \approx 2.70\%$ ) when measured by the three-point bending approach. However, this flexibility is only observed over a single crystal face, with the other two prominent faces displaying brittle behavior. Our crystal structural analyses and energy framework calculations suggest that the elastic behavior results from the quasi-isotropic interactions found within the crystal structure and the presence of herringboned layers perpendicular to the long axis of the crystal.

BCPIN results from a chemical modification to a known elastic material, (E)-1-(4-bromo-phenyl)iminomethyl-2-hydroxyl-naphthalene (BPIN). Hence, our work highlights the potential to chemically tune the optical activity of materials without adversely affecting their mechanical behavior. In accordance with the shape-synthon strategy, the incorporation of a chlorine atom (a spherical, weakly interacting synthon) into the molecular backbone drives the crystal packing towards energetically isotropic packing, which is conventional for mechanical elasticity. While the electronic structure is altered significantly from this small chemical modification, no marked change in the mechanical behavior is observed. We expect small chemical modification to become an important direction for imparting mechanical flexibility to, as well as tuning the functional properties of, molecular materials with multifunctional applications in flexible devices.

**Supplementary Materials:** CCDC 2117266 contains the supplementary crystallographic data for this paper in CIF format. These data can be obtained free of charge from The Cambridge Crystallographic Data Centre. The following are available online at <https://www.mdpi.com/article/10.3390/cryst1111397/s1>. Figure S1. Experimental (black line) and simulated (red line) PXRD patterns of BCPIN. Figure S2. Differential scanning calorimetry measurement of BCPIN. Figure S3. Face indexed image of pristine crystal of BCPIN. Table S1. Crystallographic and structural refinement parameters of BCPIN. Figure S4. Thermal ellipsoid drawing of the asymmetric unit of BCPIN showing atom labels and 50% probability of ellipsoids. Figure S5. Visualization of energy frameworks showing electrostatic (red), dispersion (green) components and total interaction energy (blue) for BCPIN, in the (a) (001), (b) (100) and (c) (010) faces, respectively. The energy scale factor is  $100 \text{ kJ}\cdot\text{mol}^{-1}$  and the energy threshold is  $10 \text{ kJ}\cdot\text{mol}^{-1}$ . Table S2. Molecular structure pairs and the interaction energies ( $\text{kJ}\cdot\text{mol}^{-1}$ ) obtained from energy frameworks calculation for BCPIN. Scale factors are in the lower table. Figure S6. Microscopic image of bended BCPIN crystal. The elastic strain was calculated according to the Euler-Bernoulli equation  $\epsilon = t/d$  ( $t$  = beam thickness;  $d$  = diameter of curvature). The observed elastic stress before breaking is 2.70%.

**Author Contributions:** B.B. and A.A.L.M. conceived and designed the experiments. T.F. and B.B. synthesized and characterized the compounds. V.S. and E.L.-K. handled the photoluminescence studies. A.A.L.M. performed the computational calculations. B.B. and F.E. supervised the work. All authors have read and agreed to the published version of the manuscript.

**Funding:** B.B. acknowledges funding from Deutsche Forschungsgemeinschaft (DFG), Project No. 450137475.

**Acknowledgments:** All authors extend thanks to BAM IT for access to computational resources. This work was carried out in the framework of the Joint Lab GEN\_FAB and with the support of the Helmholtz Innovation Lab HySPRINT.

**Conflicts of Interest:** The authors declare no conflict of interest.

## References

1. Reddy, C.M.; Rama Krishna, G.; Ghosh, S. Mechanical Properties of Molecular Crystals—Applications to Crystal Engineering. *CrystEngComm* **2010**, *12*, 2296. [[CrossRef](#)]
2. Reddy, C.M.; Padmanabhan, K.A.; Desiraju, G.R. Structure–Property Correlations in Bending and Brittle Organic Crystals. *Cryst. Growth Des.* **2006**, *6*, 2720–2731. [[CrossRef](#)]
3. Bhunia, S.; Chandel, S.; Karan, S.K.; Dey, S.; Tiwari, A.; Das, S.; Kumar, N.; Chowdhury, R.; Mondal, S.; Ghosh, I.; et al. Autonomous Self-Repair in Piezoelectric Molecular Crystals. *Science* **2021**, *373*, 321–327. [[CrossRef](#)] [[PubMed](#)]
4. Krishna, G.R.; Devarapalli, R.; Lal, G.; Reddy, C.M. Mechanically Flexible Organic Crystals Achieved by Introducing Weak Interactions in Structure: Supramolecular Shape Synthons. *J. Am. Chem. Soc.* **2016**, *138*, 13561–13567. [[CrossRef](#)]
5. Ghosh, S.; Mishra, M.K. Elastic Molecular Crystals: From Serendipity to Design to Applications. *Cryst. Growth Des.* **2021**, *21*, 2566–2580. [[CrossRef](#)]
6. Liu, H.; Lu, Z.; Tang, B.; Qu, C.; Zhang, Z.; Zhang, H. A Flexible Organic Single Crystal with Plastic-Twisting and Elastic-Bending Capabilities and Polarization-Rotation Function. *Angew. Chem.* **2020**, *132*, 13044–13050. [[CrossRef](#)]
7. Feiler, T.; Bhattacharya, B.; Michalchuk, A.A.L.; Rhim, S.-Y.; Schröder, V.; List-Kratochvil, E.; Emmerling, F. Tuning the Mechanical Flexibility of Organic Molecular Crystals by Polymorphism for Flexible Optical Waveguides. *CrystEngComm* **2021**, *23*, 5815–5825. [[CrossRef](#)]
8. Gupta, P.; Allu, S.; Karothu, D.P.; Panda, T.; Nath, N.K. Organic Molecular Crystals with Dual Stress-Induced Mechanical Response: Elastic and Plastic Flexibility. *Cryst. Growth Des.* **2021**, *21*, 1931–1938. [[CrossRef](#)]
9. Arkhipov, S.G.; Losev, E.A.; Nguyen, T.T.; Rychkov, D.A.; Boldyreva, E.V. A Large Anisotropic Plasticity of L-leucinium Hydrogen Maleate Preserved at Cryogenic Temperatures. *Acta Cryst.* **2019**, *B75*, 143–151. [[CrossRef](#)] [[PubMed](#)]
10. Bhattacharya, B.; Michalchuk, A.A.L.; Silbernagl, D.; Rautenberg, M.; Schmid, T.; Feiler, T.; Reimann, K.; Ghalgaoui, A.; Sturm, H.; Paulus, B.; et al. A Mechanistic Perspective on Plastically Flexible Coordination Polymers. *Angew. Chem. Int. Ed.* **2020**, *59*, 5557–5561. [[CrossRef](#)]
11. Annadhasan, M.; Agrawal, A.R.; Bhunia, S.; Pradeep, V.V.; Zade, S.S.; Reddy, C.M.; Chandrasekar, R. Mechanophotonics: Flexible Single-Crystal Organic Waveguides and Circuits. *Angew. Chem. Int. Ed.* **2020**, *59*, 13852–13858. [[CrossRef](#)] [[PubMed](#)]
12. Annadhasan, M.; Karothu, D.P.; Chinnasamy, R.; Catalano, L.; Ahmed, E.; Ghosh, S.; Naumov, P.; Chandrasekar, R. Micromanipulation of Mechanically Compliant Organic Single-Crystal Optical Microwaveguides. *Angew. Chem. Int. Ed.* **2020**, *59*, 13821–13830. [[CrossRef](#)]
13. Bhattacharya, B.; Roy, D.; Dey, S.; Puthuvakkal, A.; Bhunia, S.; Mondal, S.; Chowdhury, R.; Bhattacharya, M.; Mandal, M.; Manoj, K.; et al. Mechanical-Bending-Induced Fluorescence Enhancement in Plastically Flexible Crystals of a GFP Chromophore Analogue. *Angew. Chem.* **2020**, *132*, 20050–20055. [[CrossRef](#)]
14. Hayashi, S.; Yamamoto, S.; Takeuchi, D.; Ie, Y.; Takagi, K. Creating Elastic Organic Crystals of  $\pi$ -Conjugated Molecules with Bending Mechanofluorochromism and Flexible Optical Waveguide. *Angew. Chem. Int. Ed.* **2018**, *57*, 17002–17008. [[CrossRef](#)] [[PubMed](#)]
15. Adler-Abramovich, L.; Arnon, Z.A.; Sui, X.; Azuri, I.; Cohen, H.; Hod, O.; Kronik, L.; Shimon, L.J.W.; Wagner, H.D.; Gazit, E. Bioinspired Flexible and Tough Layered Peptide Crystals. *Adv. Mater.* **2018**, *30*, 1704551. [[CrossRef](#)]
16. Wang, K.; Mishra, M.K.; Sun, C.C. Exceptionally Elastic Single-Component Pharmaceutical Crystals. *Chem. Mater.* **2019**, *31*, 1794–1799. [[CrossRef](#)]
17. Liu, H.; Lu, Z.; Zhang, Z.; Wang, Y.; Zhang, H. Highly Elastic Organic Crystals for Flexible Optical Waveguides. *Angew. Chem. Int. Ed.* **2018**, *57*, 8448–8452. [[CrossRef](#)]
18. Catalano, L.; Karothu, D.P.; Schramm, S.; Ahmed, E.; Rezgüi, R.; Barber, T.J.; Famulari, A.; Naumov, P. Dual-Mode Light Transduction through a Plastically Bendable Organic Crystal as an Optical Waveguide. *Angew. Chem. Int. Ed.* **2018**, *57*, 17254–17258. [[CrossRef](#)]
19. Naim, K.; Singh, M.; Sharma, S.; Nair, R.V.; Venugopalan, P.; Chandra Sahoo, S.; Neelakandan, P.P. Exceptionally Plastic/Elastic Organic Crystals of a Naphthalidenimine-Boron Complex Show Flexible Optical Waveguide Properties. *Chem. Eur. J.* **2020**, *26*, 11979–11984. [[CrossRef](#)]
20. Cao, J.; Liu, H.; Zhang, H. An Optical Waveguiding Organic Crystal with Phase-Dependent Elasticity and Thermoplasticity over Wide Temperature Ranges. *CCS Chem* **2020**, *2*, 2569–2575. [[CrossRef](#)]
21. Saha, S.; Mishra, M.K.; Reddy, C.M.; Desiraju, G.R. From Molecules to Interactions to Crystal Engineering: Mechanical Properties of Organic Solids. *Acc. Chem. Res.* **2018**, *51*, 2957–2967. [[CrossRef](#)]
22. Ghosh, S.; Reddy, C.M. Elastic and Bendable Caffeine Cocrystals: Implications for the Design of Flexible Organic Materials. *Angew. Chem.* **2012**, *51*, 10319–10323. [[CrossRef](#)] [[PubMed](#)]
23. Thompson, A.J.; Chamorro Orué, A.I.; Nair, A.J.; Price, J.R.; McMurtrie, J.; Clegg, J.K. Elastically Flexible Molecular Crystals. *Chem. Soc. Rev.* **2021**, *50*, 11725–11740. [[CrossRef](#)] [[PubMed](#)]



24. Karothu, D.P.; Dushaq, G.; Ahmed, E.; Catalano, L.; Rasras, M.; Naumov, P. Multifunctional Deformable Organic Semiconductor Single Crystals. *Angew. Chem. Int. Ed.* **2021**. [[CrossRef](#)]
25. Kwon, T.; Koo, J.Y.; Choi, H.C. Highly Conducting and Flexible Radical Crystals. *Angew. Chem. Int. Ed.* **2020**, *59*, 16436–16439. [[CrossRef](#)]
26. Ravi, J.; Kumar, A.V.; Karothu, D.P.; Annadhasan, M.; Naumov, P.; Chandrasekar, R. Geometrically Reconfigurable, 2D, All-Organic Photonic Integrated Circuits Made from Two Mechanically and Optically Dissimilar Crystals. *Adv. Funct. Mater.* **2021**, *31*, 2105415. [[CrossRef](#)]
27. Panda, M.K.; Ghosh, S.; Yasuda, N.; Moriwaki, T.; Mukherjee, G.D.; Reddy, C.M.; Naumov, P. Spatially Resolved Analysis of Short-Range Structure Perturbations in a Plastically Bent Molecular Crystal. *Nat. Chem.* **2015**, *7*, 65–72. [[CrossRef](#)]
28. Liu, X.; Michalchuk, A.A.L.; Bhattacharya, B.; Yasuda, N.; Emmerling, F.; Pulham, C.R. High-Pressure Reversibility in a Plastically Flexible Coordination Polymer Crystal. *Nat. Commun.* **2021**, *12*, 3871. [[CrossRef](#)] [[PubMed](#)]
29. Owczarek, M.; Hujak, K.A.; Ferris, D.P.; Prokofjevs, A.; Majerz, I.; Szklarz, P.; Zhang, H.; Sarjeant, A.A.; Stern, C.L.; Jakubas, R.; et al. Flexible Ferroelectric Organic Crystals. *Nat. Commun.* **2016**, *7*, 13108. [[CrossRef](#)] [[PubMed](#)]
30. Chu, X.; Lu, Z.; Tang, B.; Liu, B.; Ye, K.; Zhang, H. Engineering Mechanical Compliance of an Organic Compound toward Flexible Crystal Lasing Media. *J. Phys. Chem. Lett.* **2020**, *11*, 5433–5438. [[CrossRef](#)]
31. Nath, N.K.; Hazarika, M.; Gupta, P.; Ray, N.R.; Paul, A.K.; Nauha, E. Plastically Bendable Crystals of Probenecid and Its Cocrystal with 4,4'-Bipyridine. *J. Mol. Struct.* **2018**, *1160*, 20–25. [[CrossRef](#)]
32. Devarapalli, R.; Kadambi, S.B.; Chen, C.-T.; Krishna, G.R.; Kammari, B.R.; Buehler, M.J.; Ramamurty, U.; Reddy, C.M. Remarkably Distinct Mechanical Flexibility in Three Structurally Similar Semiconducting Organic Crystals Studied by Nanoindentation and Molecular Dynamics. *Chem. Mater.* **2019**, *31*, 1391–1402. [[CrossRef](#)]
33. Ghosh, S.; Mishra, M.K.; Kadambi, S.B.; Ramamurty, U.; Desiraju, G.R. Designing Elastic Organic Crystals: Highly Flexible Polyhalogenated *N*-Benzylideneanilines. *Angew. Chem.* **2015**, *127*, 2712–2716. [[CrossRef](#)]
34. Ravi, J.; Annadhasan, M.; Kumar, A.V.; Chandrasekar, R. Mechanically Reconfigurable Organic Photonic Integrated Circuits Made from Two Electronically Different Flexible Microcrystals. *Adv. Funct. Mater.* **2021**, *31*, 2100642. [[CrossRef](#)]
35. Sheldrick, G.M. A Short History of SHELX. *Acta Cryst. A Found Cryst.* **2008**, *64*, 112–122. [[CrossRef](#)]
36. Sheldrick, G. *SADABS 2.03*; University of Göttingen: Göttingen, Germany, 2002.
37. Sheldrick, G.M. SHELXT—Integrated Space-Group and Crystal-Structure Determination. *Acta Cryst. A Found. Adv.* **2015**, *71*, 3–8. [[CrossRef](#)]
38. Sheldrick, G.M. Crystal Structure Refinement with SHELXL. *Acta Cryst. C Struct. Chem.* **2015**, *71*, 3–8. [[CrossRef](#)] [[PubMed](#)]
39. Dovesi, R.; Erba, A.; Orlando, R.; Zicovich-Wilson, C.M.; Civalieri, B.; Maschio, L.; Rérat, M.; Casassa, S.; Baima, J.; Salustro, S.; et al. Quantum-mechanical Condensed Matter Simulations with CRYSTAL. *WIREs Comput. Mol. Sci.* **2018**, *8*, e1360. [[CrossRef](#)]
40. Vilela Oliveira, D.; Laun, J.; Peintinger, M.F.; Bredow, T. BSSE-correction Scheme for Consistent Gaussian Basis Sets of Double- and Triple-zeta Valence with Polarization Quality for Solid-state Calculations. *J. Comput. Chem.* **2019**, *40*, 2364–2376. [[CrossRef](#)]
41. Heyd, J.; Peralta, J.E.; Scuseria, G.E.; Martin, R.L. Energy Band Gaps and Lattice Parameters Evaluated with the Heyd-Scuseria-Ernzerhof Screened Hybrid Functional. *J. Chem. Phys.* **2005**, *123*, 174101. [[CrossRef](#)]
42. Michalchuk, A.A.L.; Trestman, M.; Rudić, S.; Portius, P.; Fincham, P.T.; Pulham, C.R.; Morrison, C.A. Predicting the Reactivity of Energetic Materials: An *Ab Initio* Multi-Phonon Approach. *J. Mater. Chem. A* **2019**, *7*, 19539–19553. [[CrossRef](#)]
43. Spackman, P.R.; Turner, M.J.; McKinnon, J.J.; Wolff, S.K.; Grimwood, D.J.; Jayatilaka, D.; Spackman, M.A. *CrystalExplorer: A Program for Hirshfeld Surface Analysis, Visualization and Quantitative Analysis of Molecular Crystals*. *J. Appl. Cryst.* **2021**, *54*, 1006–1011. [[CrossRef](#)] [[PubMed](#)]
44. Turner, M.J.; Thomas, S.P.; Shi, M.W.; Jayatilaka, D.; Spackman, M.A. Energy Frameworks: Insights into Interaction Anisotropy and the Mechanical Properties of Molecular Crystals. *Chem. Commun.* **2015**, *51*, 3735–3738. [[CrossRef](#)] [[PubMed](#)]
45. Thomas, S.P.; Shi, M.W.; Koutsantonis, G.A.; Jayatilaka, D.; Edwards, A.J.; Spackman, M.A. The Elusive Structural Origin of Plastic Bending in Dimethyl Sulfone Crystals with Quasi-isotropic Crystal Packing. *Angew. Chem. Int. Ed.* **2017**, *56*, 8468–8472. [[CrossRef](#)]